systems

MDPI

Article

A Compact Filtering Coupler with Unwanted Harmonic Rejection Using LC Composite Lines for Communication Systems Applications

Saeed Roshani [1], Salah I. Yahya [2,3], Yaqeen Sabah Mezaal [4], Muhammad Akmal Chaudhary [5], Aqeel A. Al-Hilali [6], Yazeed Yasin Ghadi [7], Mohsen Karimi [1] and Sobhan Roshani [1,*]

1 Department of Electrical Engineering, Kermanshah Branch, Islamic Azad University, Kermanshah 67146, Iran
2 Department of Communication and Computer Engineering, Cihan University-Erbil, Erbil 44001, Iraq
3 Department of Software Engineering, Faculty of Engineering, Koya University, Koya KOY45, Iraq
4 Medical Instrumentation Engineering Department, Al-Esraa University College, Baghdad 10071, Iraq
5 College of Engineering and Information Technology, Ajman University, Ajman P.O. Box 346, United Arab Emirates
6 College of Medical Techniques, Al-Farahidi University, Baghdad PXW+7995, Iraq
7 Software Engineering and Computer Science Department, Al Ain University, Al Ain 15551, United Arab Emirates
* Correspondence: s.roshani@aut.ac.ir

Abstract: In this paper, new LC lumped components and composite lines are used to create a filtering branch line coupler (FBLC) with a small size and wide suppression band. New composite lines are proposed using applied LC lumped components, which are used as the coupler main branches. The proposed FBLC suppresses second to sixth harmonics with high attention level and provides a wide stopband from 1.6 GHz to 5 GHz with more than 20 dB of attention. The presented coupler is analyzed, designed, simulated, and implemented. The measured results show that the proposed FBLC correctly operates at 800 MHz with less than 0.25 dB of insertion loss. In addition, more than 29 dB of return loss and isolation is measured at operating frequency, which shows the correct performance of the proposed design. The size of the proposed FBLC is equal to 23.7 mm × 25.5 mm (0.086λ × 0.093λ), which shows an 87% size reduction. The proposed FBLC with the designed frequency can be used in the communication systems for narrow-band Internet of things (NB-IoT) and traffic control radar applications.

Keywords: filtering coupler; harmonic rejection; composite line; communication systems; NB-IoT

Citation: Roshani, S.; Yahya, S.I.; Mezaal, Y.S.; Chaudhary, M.A.; Al-Hilali, A.A.; Ghadi, Y.Y.; Karimi, M.; Roshani, S. A Compact Filtering Coupler with Unwanted Harmonic Rejection Using LC Composite Lines for Communication Systems Applications. *Systems* **2023**, *11*, 14. https://doi.org/10.3390/systems11010014

Academic Editor: Paolo Visconti

Received: 2 December 2022
Revised: 22 December 2022
Accepted: 27 December 2022
Published: 29 December 2022

1. Introduction

The branch line couplers (BLCs) are widely used components in microwave and RF circuits, which have different types such as branch line, hybrid, and rat race. The coupler devices are commonly being used in balanced power amplifiers [1], Doherty power amplifiers [2,3], array antennas [4,5], and phase shifters [6]. Conventional BLCs are composed of four λ/4 transmission lines (TLs), which occupy a large area. Moreover, another disadvantage of the conventional couplers is that there is no suppression band in these devices, which cannot suppress the undesirable signals at unwanted frequencies. Several approaches have been presented to improve the performance and solve the conventional coupler disadvantages, which are explained in what follows.

A dual-band coupler is designed with coupled lines in [7], operating at 1.8 GHz and 0.9 GHz; however, the designed coupler has a large size. In [8], a differential coupler using a coupled line structure is designed with long parallel coupled lines. High insertion loss and rather large size are disadvantages in the designed coupler in [8].

Resonators, which can improve the performance of the electronic components [9], are widely used to provide a wide suppression band for the microwave devices, such

as couplers [10], filters [11,12], and diplexers [13]. FBLC is designed using resonators in [14] and meandered lines to decrease the area and increase the performance of the device. According to the results in [14], the meandered lines have reduced the length of the coupler's main branches; moreover, the applied resonators and open stubs have created transmission zeros to provide a suppression band for the coupler. A rat-race coupler (RRC) is designed in [15], in which capacitive open stubs and T-shaped resonators are incorporated to present an RRC with reduced size and high performance. The E-shaped impedance transformer is used in [16] to design a dual-band coupler with high frequency ratio. Open stubs are also used in [16] to create desired transmission zeros. In [17], capacitive open stubs are applied in the BLC structure to achieve compact size, but the obtained insertion loss is high. Open stubs and resonators can be used together in the BLC structure to obtain high performances of the device [18].

The electromagnetic bandgap (EBG) has also been used in the design of the microwave devices, such as couplers to reduce the size or to improve the functionality of the devices. However, the EBG method increases the design and fabrication complexity. Substrate-integrated gap waveguide (SIGW) and EBG methods are used for designing of a wideband coupler in [19]; however, the obtained coupler has a large size. Couplers are also designed using a photonic crystal for higher frequencies [20–25].

Recently, artificial neural network (ANN) techniques and optimization algorithms [26,27] have helped electronics designers to improve the performances of their devices [28–32], which also have been used in the designing of the couplers [33–35]. In [33], a feedforward network was used to predict the BLC transfer function. By using the transfer function, the locations of the transmission zeros can be obtained, which help to design the coupler with desired specifications. In [36], a neural network and the back propagation method with Bayesian regularization are used to improve the filters' performance. In addition, a feedforward ANN is used in [37] to design a power divider with reduced size. A combination of ANNs and optimization algorithms is also used together to present a design method for amplifier design in [38].

Recently, lumped elements have been used in coupler designs for achieving a miniaturized size or filtering response [39]. Capacitors are used in [40] to create a compact coupler with suppression of harmonics; however, the obtained operating band is very narrow, which may be because of frequency shifting in the fabrication. In addition, varactor diodes can be used in the coupler structure, which can provide tunable and reconfigurable performance of the coupler [41]. Capacitors and inductors are used in the coupler structure designed in [42], but the obtained insertion losses in the output ports are high.

In this paper, lumped components, four capacitors, and four inductors are used with transmission lines to create composite lines to design a branch line coupler, which has resulted in improvement of coupler performances, such as miniaturized size and wide suppression band. The achieved suppression band of the device has helped to attenuate the unwanted frequencies, such as undesired harmonics.

2. Design Process

In this section, the design process of the typical and proposed couplers is explained as follows.

2.1. Typical 800 MHz Coupler

The structure of the typical 0.8 GHz FBLC is shown in Figure 1, which consists of four $\lambda/4$ branches. With the applied RT-Duroid 5880 substrate (ε_r = 2.2 and 20 mil thickness), the size of the typical coupler is 71.1 mm $\times$ 69.8 mm. Large occupied size is the first drawback of this coupler.

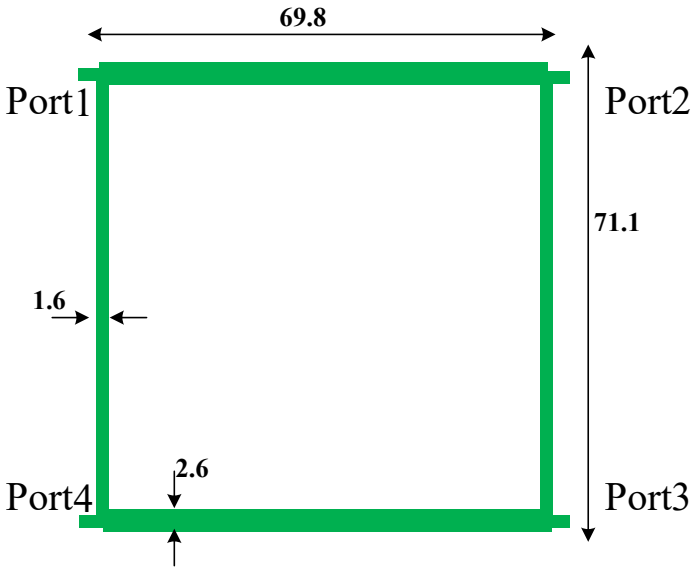

Figure 1. The structure of the typical 0.8 GHz FBLC. All dimensions are written in mm unit.

The typical 800 MHz FBLC frequency response is depicted in Figure 2. The amplitudes of S_{12} and S_{13} are −3.1 dB and −3.2 dB, which shows less than 0.2 dB insertion loss at operating frequency. The amplitude of S_{11} is about −32 dB, and the amplitude of S_{14} is about −36 dB, which shows good performance of the typical coupler at operating frequency. A typical FBLC has good performance at operating frequency, but the performance of this coupler at higher frequency is not acceptable, and undesirable signals are passed, without any suppression at higher frequencies, which is another drawback of the typical FBLC.

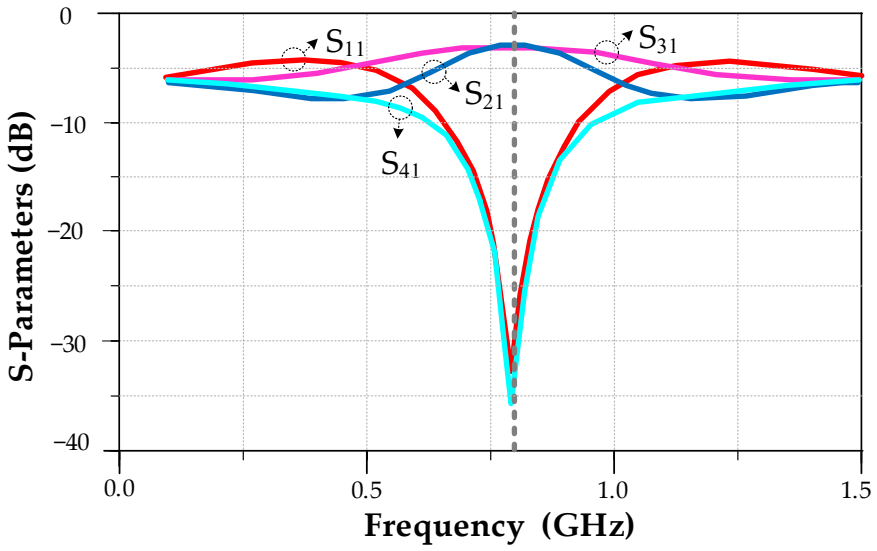

Figure 2. The S-parameters of the typical 0.8 GHz FBLC.

2.2. Proposed Coupler

As mentioned in the previous section, the typical FBLC has two main drawbacks. Firstly, it has a large size, and secondly it passes undesirable signals at higher frequencies such as the main signal without any suppression. In order to overcome these drawbacks, a proposed structure is presented in Figure 3, in which four lumped inductors and four capacitors are used.

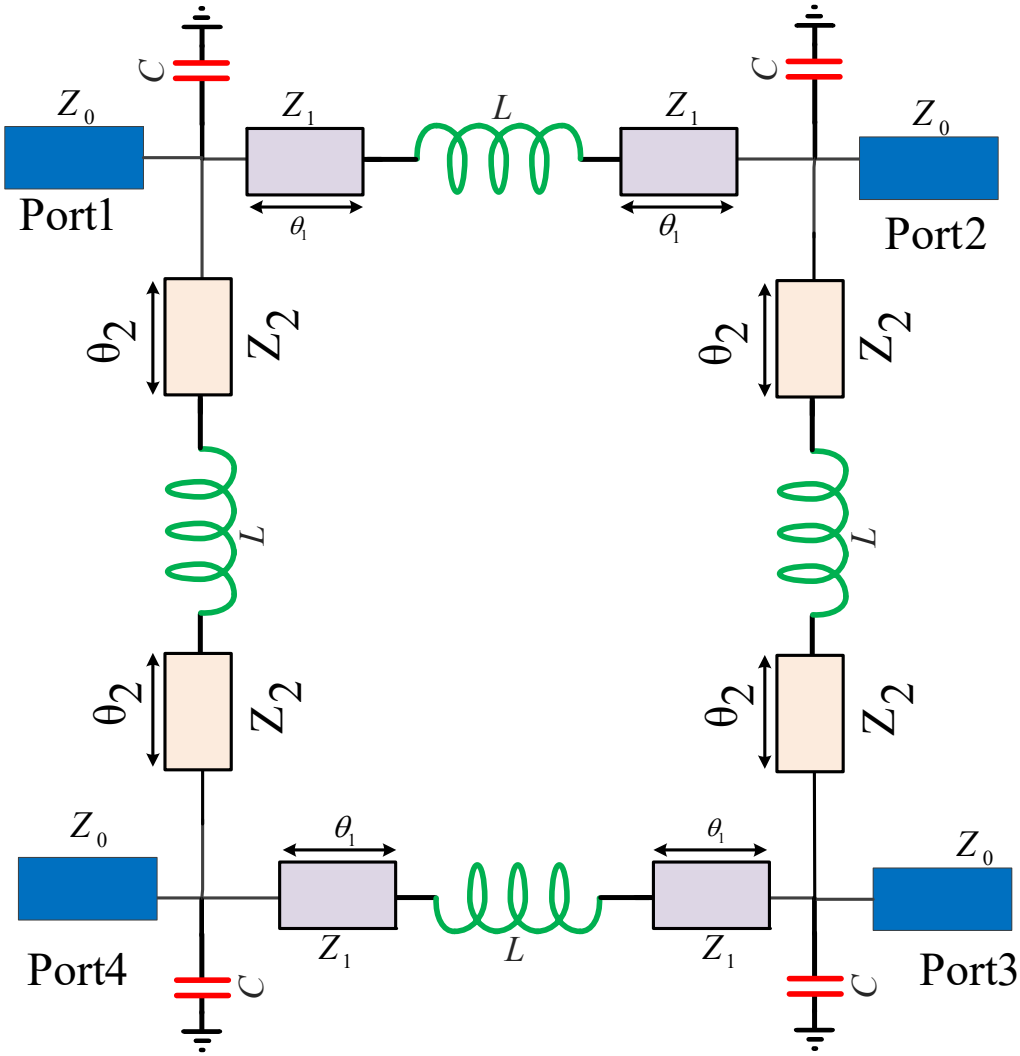

Figure 3. The structure of the proposed 0.8 GHz FBLC.

3. Proposed FBLC Analysis

In the conventional coupler, four long branches are used, which occupies large area, so the length reduction of these branches is an important parameter to miniaturize the device [43]. In the proposed FBLC, two types of composite lines are used instead of two long conventional branches. In Figure 4a, the conventional horizontal branch is depicted, which has 90 degrees of length and has 35.5 ohms of impedance. In the proposed coupler, a new horizontal composite branch is proposed as depicted in Figure 4b, which is applied instead of the long conventional branch. These two lines must have the same performance at an operating frequency of 800 MHz. As mentioned, the proposed branches not only reduce the size of the device but also improve the performance of the frequency response. The scattering parameters of the conventional horizontal $\lambda/4$ line and the proposed compact horizontal TL are compared in Figure 4c. As seen, both lines have the same insertion loss of 0.05 dB at the 0.8 GHz operating frequency. The proposed horizontal transmission line provides a wide suppression band, while the conventional TL does not provide any harmonics suppression.

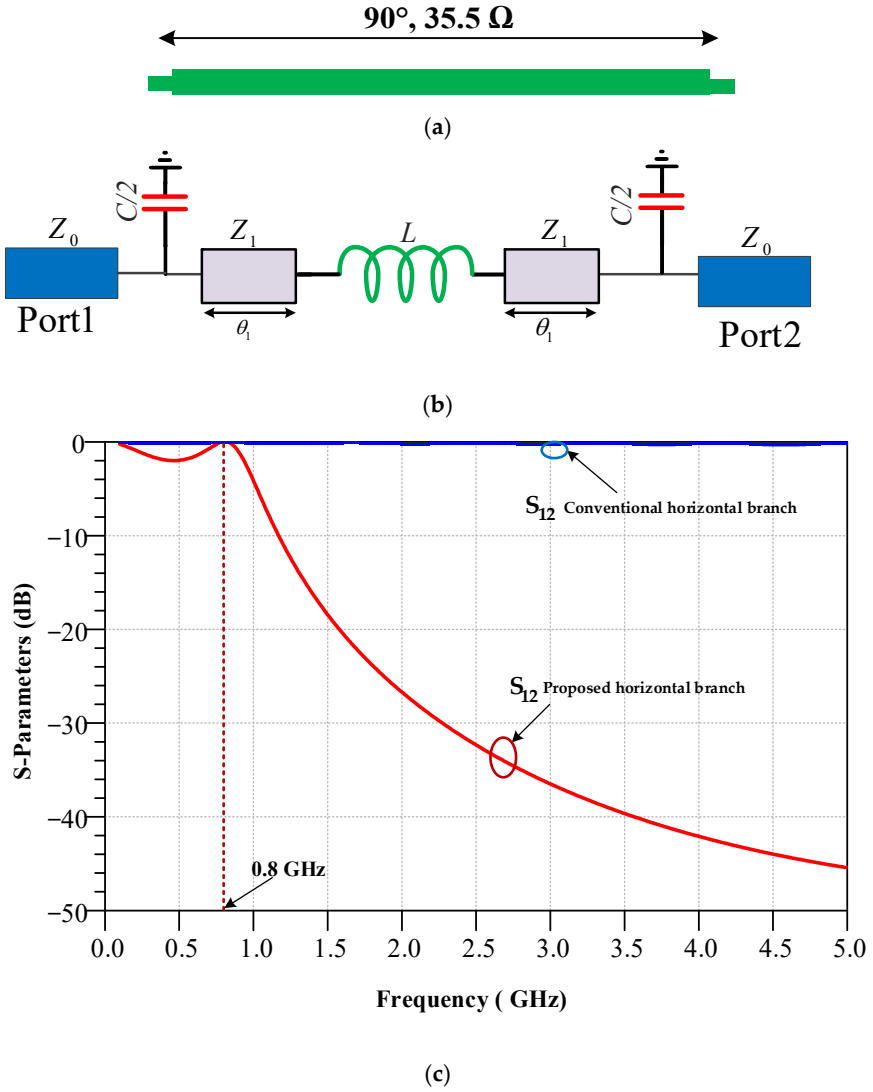

Figure 4. The (**a**) conventional and (**b**) proposed horizontal branches of the coupler. (**c**) The S-parameters' results.

The ABCD parameters for the conventional and the proposed horizontal branches should be equated as written in Equation (1):

$$\begin{aligned}&[M\_ABCD\_C] \times [M\_ABCD\_TL] \times [M\_ABCD\_L] \times \\ &[M\_ABCD\_TL] \times [M\_ABCD\_C] \\ &= [M\_ABCD\_BR]\end{aligned} \tag{1}$$

wherein (1) *M_ABCD_C* is the ABCD matrix of the capacitor. Moreover, *M_ABCD_TL*, *M_ABCD_L*, and *M_ABCD_BR* are ABCD matrices of the transmission line, inductor, and conventional 90-degree branch line, respectively. The ABCD matrices are defined in Equations (2)–(5) as follows [44]:

$$[M\_ABCD\_C] = \begin{pmatrix} 1 & 0 \\ \frac{C\omega \mathrm{i}}{2} & 1 \end{pmatrix} \tag{2}$$

$$[M\_ABCD\_TL] = \begin{pmatrix} \cos(\theta_1) & Z_1 \sin(\theta_1)\mathrm{i} \\ \frac{\sin(\theta_1)\mathrm{i}}{Z_1} & \cos(\theta_1) \end{pmatrix} \tag{3}$$

$$[M\_ABCD\_L] = \begin{pmatrix} 1 & L\omega\mathrm{i} \\ 0 & 1 \end{pmatrix} \tag{4}$$

where $\omega = 2\pi f$. After simplifying Equations (1)–(4), the final equation can be calculated as written in Equation (5):

$$\begin{pmatrix} \cos(\theta_1)^2 + \frac{C\omega\sigma_1\mathrm{i}}{2} + \frac{\sin(\theta_1)(Z_1\sin(\theta_1)\mathrm{i}+L\omega\cos(\theta_1)\mathrm{i})\mathrm{i}}{Z_1} & \sigma_1 \\ \cos(\theta_1)\sigma_4 + \frac{\sin(\theta_1)\sigma_3\mathrm{i}}{Z_1} + \frac{C\omega\sigma_2\mathrm{i}}{2} & \sigma_2 \end{pmatrix} = \begin{pmatrix} 0 & jZ_{BR} \\ jY_{BR} & 0 \end{pmatrix} \tag{5}$$

where the values of σ_1–σ_4 are defined in Equations (6)–(9) as the following:

$$\sigma_1 = \cos(\theta_1)(Z_1\sin(\theta_1)\mathrm{i} + L\omega\cos(\theta_1)\mathrm{i}) + Z_1\cos(\theta_1)\sin(\theta_1)\mathrm{i} \tag{6}$$

$$\sigma_2 = \cos(\theta_1)\sigma_3 + Z_1\sin(\theta_1)\sigma_4\mathrm{i} \tag{7}$$

$$\sigma_3 = \cos(\theta_1) - \frac{CZ_1\omega\sin(\theta_1)}{2} + Lw\sigma_4\mathrm{i} \tag{8}$$

$$\sigma_4 = \frac{\sin(\theta_1)\mathrm{i}}{Z_1} + \frac{C\omega\cos(\theta_1)\mathrm{i}}{2} \tag{9}$$

Equation (5) has an infinite number of solutions. Therefore, some assumptions should be considered for calculating this equation. The values of capacitors (C) and inductors (L) are considered as written in Table 1. Moreover, the values of Z_1 and θ_1 are calculated based on Equation (5) and the desired size reduction. The value of applied stubs and lumped elements components is listed in the Table 1.

Table 1. The obtained value of applied stubs and lumped elements components.

L	C	Z_1	θ_1	Z_2	θ_2
6 nH	5.2 pF	10 Ω	15°	161 Ω	5°

In Figure 5a, the conventional vertical branch is depicted, which has 90 degrees of length and has 50 ohms of impedance. In the proposed coupler, a new vertical composite branch is proposed as depicted in Figure 5b, which is applied instead of the long conventional branch. These two lines must have the same performance at an operating frequency of 800 MHz. The scattering parameters of the conventional vertical λ/4 line and the proposed compact vertical TL are compared in Figure 5c. As seen, both lines have the same values of insertion loss of 0.05 dB at the 0.8 GHz operating frequency. Moreover, the proposed vertical transmission line provides a wide suppression band, while conventional TL cannot provide any harmonics suppression.

Similar to the horizontal analyses, the ABCD parameters for the conventional and the proposed vertical branches should be equated using Equations (1)–(9). The values of Z_2 and θ_2 are calculated as listed in Table 1.

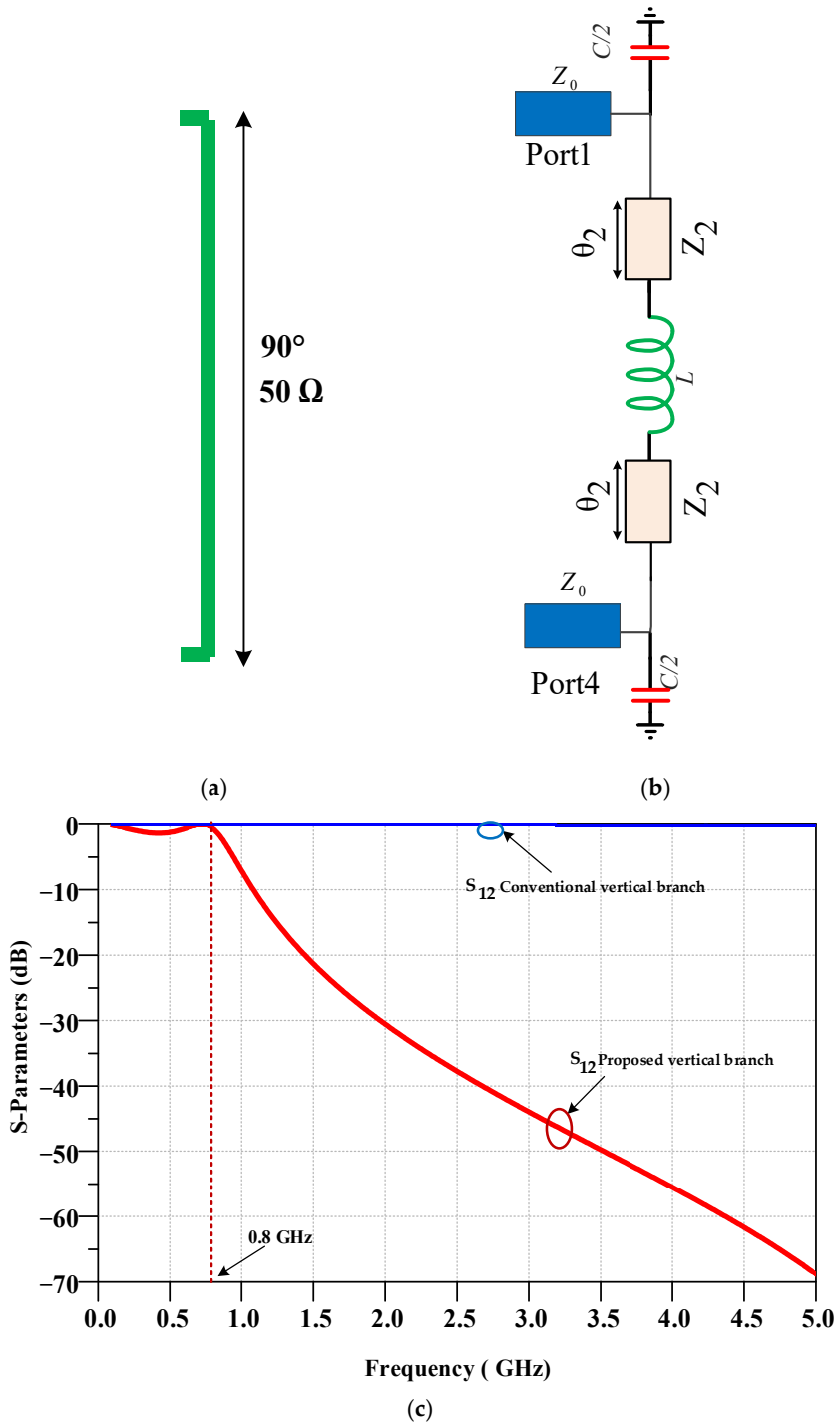

Figure 5. The (**a**) conventional and (**b**) proposed vertical branches of the coupler. (**c**) The S-parameters' results.

4. Simulations

In the design of the proposed FBLC, Duroid 5880 substrate is applied. The layout of the proposed FBLC is illustrated in Figure 6. The proposed FBLC only occupied 23.7 mm × 25.5 mm (0.086λ × 0.093λ), which shows 87% size reduction compared with the conventional coupler. As seen from Figure 6, Z_1 and θ_1, which correspond to the horizontal branches of the coupler, are shown in the coupler layout. Moreover, Z_2 and θ_2, which correspond to the vertical branches of the coupler, are indicated in the coupler layout. The values of the Z_1, θ_1, Z_2, and θ_2 are calculated based on the extracted analyses of the coupler,

which are explained in Section 3, and the obtained values are listed in Table 1. By using the obtained values for Z_1, θ_1, Z_2, and θ_2, the microstrip realization of these transmission lines and also the layout of the proposed coupler can be extracted as shown in Figure 6. The simulation's result of the proposed FBLC is illustrated in Figure 7. The proposed FBLC has good performance at the operating frequency and higher frequency bands. The amplitudes of S_{12} and S_{13} are −3.05 dB and −3.01 dB, which shows less than 0.05 dB of insertion loss at the operating frequency in simulation. The amplitude of S_{11} is about −23 dB, and the amplitude of S_{14} is about −41 dB, which shows desirable performance for the simulated proposed FBLC. At higher frequencies, the proposed coupler suppresses second to sixth harmonics with a high attention level and provides a wide rejection band from 1.6 GHz to 5 GHz with more than 20 dB of attention.

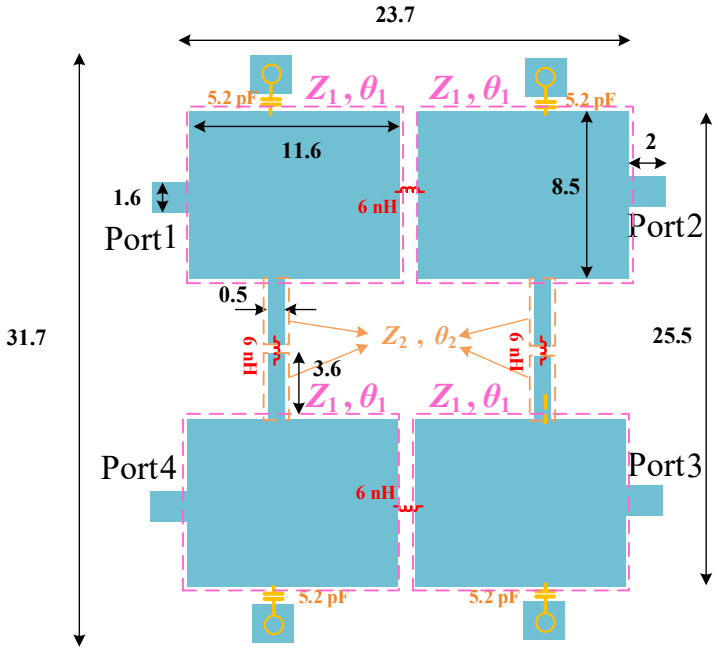

Figure 6. The layout of the proposed 0.8 GHz FBLC. All dimensions are written in mm unit. Via holes, which are used in the layout, are indicated with 4 circles at upper and lower sections of the device.

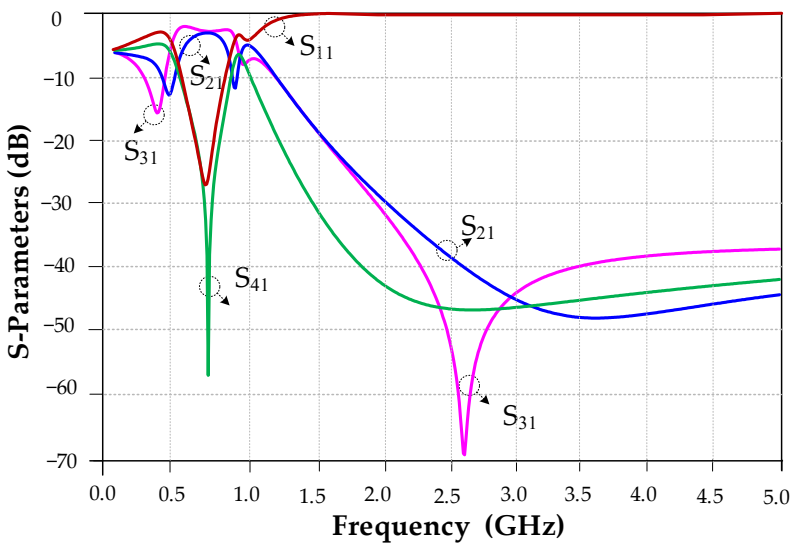

Figure 7. The simulation result of the presented 0.8 GHz FBLC.

The effects of capacitors and the inductors' result in the presented LC branches of the designed 0.8 GHz FBLC are shown in Figure 8. As seen, by tuning the values of capacitors and inductors in the presented LC branches, the operating frequency and the operating bandwidth can be adjusted.

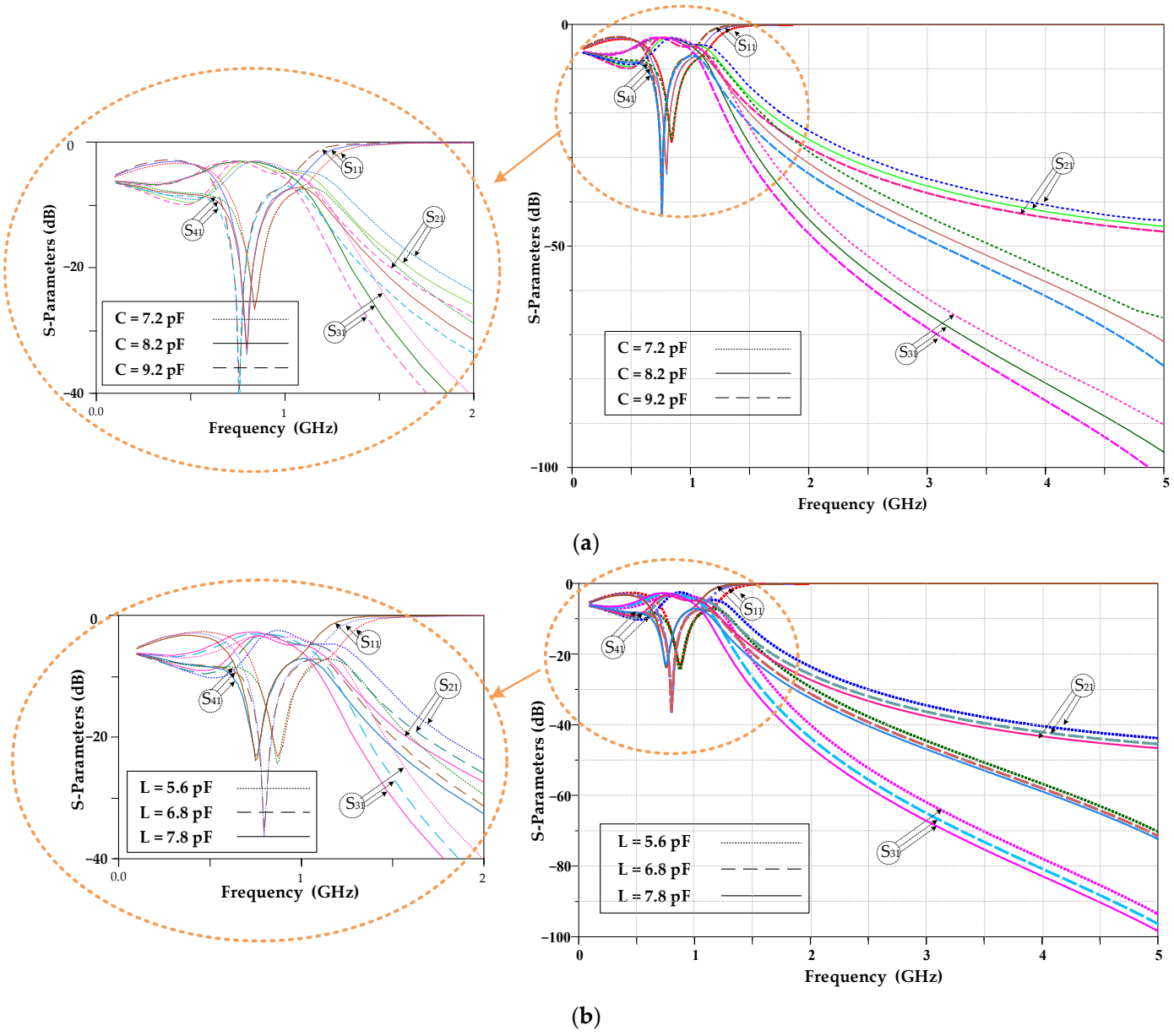

Figure 8. The effects of (**a**) capacitors and (**b**) inductors' result in the presented LC branches of the designed 0.8 GHz FBLC.

The output ports' phase difference of the presented FBLC is depicted in Figure 9. As seen, the output ports' phase difference of the designed coupler is equal to −270.12°, at the operating frequency of 800 MHz, which is so close to the ideal value.

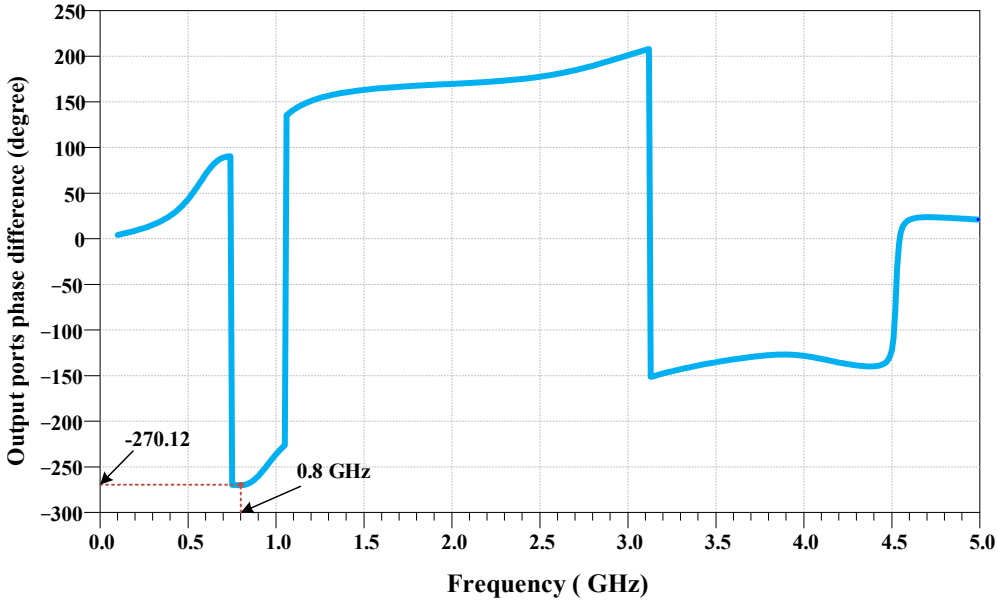

Figure 9. The output ports' phase difference of the presented 0.8 GHz FBLC.

5. Fabrication

The proposed FBLC was measured and fabricated, which is depicted in Figure 10. As seen in the fabricated device, four capacitors and four inductors are soldered on the layout. The fabricated device has a small size of 23.7 mm × 25.5 mm (0.086λ × 0.093λ), which shows 87% size reduction compared with the conventional coupler.

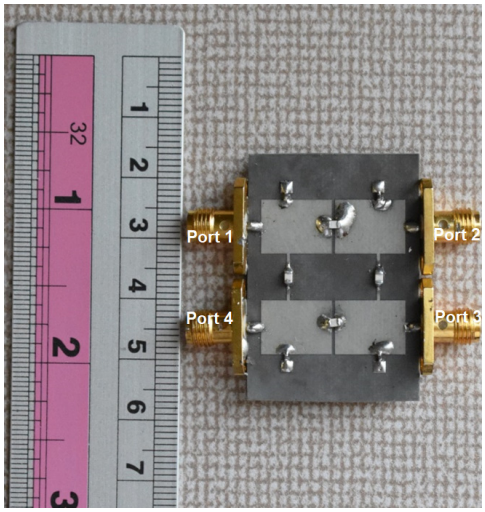

Figure 10. The fabricated prototype of the presented 0.8 GHz FBLC.

The measured result of the presented FBLC is illustrated in Figure 11. The proposed FBLC has good performance at both operating frequency and higher frequency bands. The measured amplitudes of S_{12} and S_{13} are −3.1 dB and −3.25 dB, which shows less than 0.25 dB of insertion loss at operating frequency. The measured amplitude of S_{11} is about −29 dB, and the amplitude of S_{14} is about −28 dB, which shows desirable performance for the fabricated proposed FBLC. At higher frequencies, the proposed coupler suppresses second to sixth harmonics with high attention level and provides a wide stopband from 1.6 GHz to 5 GHz with more than 20 dB of attention.

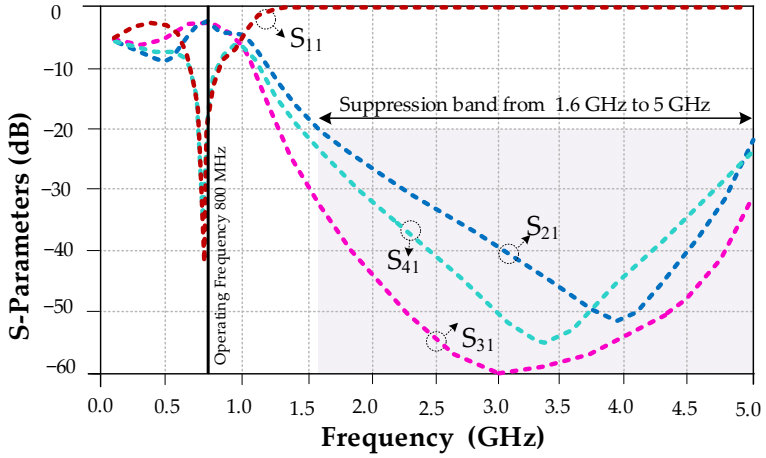

Figure 11. The measured results of the proposed 0.8 GHz FBLC.

In order to show the superiority of the proposed coupler's achieved parameters, the performances of the proposed coupler are compared with some related couplers, listed in Table 2. As shown, the proposed branches, which are used in the designed coupler, have resulted in the desired performance, compared with the other related works. Moreover, the wide rejection band and high miniaturization are achieved for the proposed coupler, while the desirable parameters of the coupler at operating frequency are obtained.

Table 2. The comparison between proposed 800 MHz branch line coupler and other related works.

Ref.	Operating Frequency (MHz)	Size Reduction	Harmonics Suppression
[45]	2400	55%	-
[46]	2000	72%	2nd and 3rd
[33]	1800	66%	2nd
[47]	1350	64%	2nd and 3rd
[48]	1160	55%	-
[49]	900	64%	3rd and 5th
[50]	835	73%	2nd
[51]	750	84%	2nd–7th
[52]	1000	73%	2nd
[15]	1800	74%	2nd–7th
[53]	1000	63%	2nd and 3rd
[54]	2400	55%	2nd and 3rd
This work	800	87%	2nd–6th

6. Conclusions

A compact FBLC with a wide suppression band is presented in this paper. In the conventional FBLC, four long, quarter wavelength branches are used, which occupy a large area. In the proposed design, lumped components and transmissions lines are used together to create new compact composite lines. The proposed composite lines are used instead of the long branches in the FBLC structure. The proposed FBLC correctly operates at 800 MHZ and rejects second to sixth harmonics with a high attention level. Moreover, the designed FBLC provides a wide stopband from 1.6 GHz to 5 GHz with more than 20 dB of attention. In the designed coupler, four inductors and four capacitors are used, which in addition to harmonics suppression also reduce the size of the device. The proposed FBLC has a size of 23.7 mm $\times$ 25.5 mm (0.086λ $\times$ 0.093λ), which shows an 87% size reduction compared with the conventional coupler. The proposed coupler is implemented on Rogers RT-Duroid substrate, and the measured result validates the correct performance of the coupler.

Author Contributions: Conceptualization, S.R. (Sobhan Roshani), S.I.Y., S.R. (Saeed Roshani) and M.K.; methodology, Y.Y.G., Y.S.M., A.A.A.-H. and S.R. (Saeed Roshani); software, M.A.C., M.K. and S.R. (Saeed Roshani); validation, M.K. and Y.Y.G.; formal analysis, S.I.Y. and S.R. (Saeed Roshani); investigation, S.R. (Saeed Roshani); resources, S.R. (Sobhan Roshani); writing—original draft preparation, S.R.(Sobhan Roshani) and S.R. (Saeed Roshani); writing—review and editing, A.A.A.-H., M.K., M.A.C., Y.Y.G., Y.S.M. and S.I.Y. All authors have read and agreed to the published version of the manuscript.

Funding: This research received no external funding.

Data Availability Statement: All the material conducted in the study is mentioned in the article.

Conflicts of Interest: The authors declare no conflict of interest.

References

1. Pednekar, P.H.; Hallberg, W.; Fager, C.; Barton, T.W. Analysis and design of a Doherty-like RF-input load modulated balanced amplifier. *IEEE Trans. Microw. Theory Tech.* **2018**, *66*, 5322–5335. [CrossRef]
2. Nikandish, G.; Staszewski, R.B.; Zhu, A. Breaking the bandwidth limit: A review of broadband Doherty power amplifier design for 5G. *IEEE Microw. Mag.* **2020**, *21*, 57–75. [CrossRef]
3. Faten, A.C. Optical design of dilute nitride quantum wells vertical cavity semiconductor optical amplifiers for communication systems. *ARO-Sci. J. Koya Univ.* **2016**, *4*, 8–12.
4. Koziel, S.; Bekasiewicz, A. Fast surrogate-assisted frequency scaling of planar antennas with circular polarisation. *IET Microw. Antennas Propag.* **2019**, *13*, 602–607. [CrossRef]
5. Yahya, S.I. Anticipated Impact of In-Car Mobile Calls on the Electromagnetic Interaction of Handset Antenna and Human. *ARO-Sci. J. Koya Univ.* **2014**, *2*, 1–10.
6. Venter, J.J.; Stander, T.; Ferrari, P. $ X $-Band Reflection-Type Phase Shifters Using Coupled-Line Couplers on Single-Layer RF PCB. *IEEE Microw. Wirel. Compon. Lett.* **2018**, *28*, 807–809. [CrossRef]
7. Wang, X.; Yin, W.-Y.; Wu, K.-L. A dual-band coupled-line coupler with an arbitrary coupling coefficient. *IEEE Trans. Microw. Theory Tech.* **2012**, *60*, 945–951. [CrossRef]
8. Martel, J.; Fernández-Prieto, A.; del Río, J.L.M.; Martín, F.; Medina, F. Design of a differential coupled-line directional coupler using a double-side coplanar waveguide structure with common-signal suppression. *IEEE Trans. Microw. Theory Tech.* **2020**, *69*, 1273–1281. [CrossRef]
9. Parandin, F.; Sheykhian, A.; Bagheri, N. A Novel Design for an Ultracompact Optical Majority Gate Based on Ring Resonator on Photonic Crystals Substrate. *J. Comput. Electron.* 2022; *under review*. [CrossRef]
10. Hosseini, S.M.; Rezaei, A. Design of a Branch-line Microstrip Coupler Using Spirals and Step Impedance Cells for WiMAX Applications. *Aro-Sci. J. Koya Univ.* **2020**, *8*, 1–4. [CrossRef]
11. Rezaei, A.; Yahya, S.I. High-performance ultra-compact dual-band bandpass filter for global system for mobile communication-850/global system for mobile communication-1900 applications. *ARO-Sci. J. Koya Univ.* **2019**, *7*, 34–37. [CrossRef]
12. Yahya, S.I.; Rezaei, A.; Khaleel, Y.A. Design and Analysis of a Wide Stopband Microstrip Dual-band Bandpass Filter. *ARO-Sci. J. Koya Univ.* **2021**, *9*, 83–90. [CrossRef]
13. Yahya, S.I.; Rezaei, A. An Area-efficient Microstrip Diplexer with a Novel Structure and Low Group Delay for Microwave Wireless Applications. *ARO-Sci. J. Koya Univ.* **2020**, *8*, 71–77. [CrossRef]
14. Hosseinkhani, F.; Roshani, S. A compact branch-line coupler design using low-pass resonators and meandered lines open stubs. *Turk. J. Electr. Eng. Comput. Sci.* **2018**, *26*, 1164–1170.
15. Lalbakhsh, A.; Mohamadpour, G.; Roshani, S.; Ami, M.; Roshani, S.; Sayem, A.S.M.; Alibakhshikenari, M.; Koziel, S. Design of a compact planar transmission line for miniaturized rat-race coupler with harmonics suppression. *IEEE Access* **2021**, *9*, 129207–129217. [CrossRef]
16. Xia, L.; Li, J.-L.; Twumasi, B.A.; Liu, P.; Gao, S.-S. Planar dual-band branch-line coupler with large frequency ratio. *IEEE Access* **2020**, *8*, 33188–33195. [CrossRef]
17. Jung, S.-C.; Negra, R.; Ghannouchi, F.M. A design methodology for miniaturized 3-dB branch-line hybrid couplers using distributed capacitors printed in the inner area. *IEEE Trans. Microw. Theory Tech.* **2008**, *56*, 2950–2953. [CrossRef]
18. Jamshidi, M.B.; Roshani, S.; Talla, J.; Mohammadi, M.S.; Roshani, S.; Peroutka, Z. A Modified Branch Line Coupler with Ultra-Wide Harmonics Rejection Using Resonators and Open-Ended Stubs. In Proceedings of the 2021 IEEE 12th Annual Ubiquitous Computing, Electronics & Mobile Communication Conference (UEMCON), New York, NY, USA, 1–4 December 2021; pp. 0860–0865.
19. Shen, D.; Wang, K.; Zhang, X. A substrate integrated gap waveguide based wideband 3-dB coupler for 5G applications. *IEEE Access* **2018**, *6*, 66798–66806. [CrossRef]
20. Askarian, A.; Parandin, F. A novel proposal for all optical 1-bit comparator based on 2D linear photonic crystal. *J. Comput. Electron.* **2022**, 1–8. [CrossRef]

21. Lalbakhsh, A.; Parandin, F.; Parandin, F.; Kamarian, R.; Jomour, M.; Alibakhshikenari, M. Ultra-compact photonic crystal based all optical half adder. In *2021 Photonics & Electromagnetics Research Symposium (PIERS)*; IEEE: Hangzhou, China, 2021.
22. Parandin, F.; Heidari, F.; Rahimi, Z.; Olyaee, S. Two-Dimensional photonic crystal Biosensors: A review. *Opt. Laser Technol.* **2021**, *144*, 107397. [CrossRef]
23. Parandin, F.; Kamarian, R.; Jomour, M. A novel design of all optical half-subtractor using a square lattice photonic crystals. *Opt. Quantum Electron.* **2021**, *53*, 114. [CrossRef]
24. Karkhanehchi, M.M.; Parandin, F.; Zahedi, A. Design of an all optical half-adder based on 2D photonic crystals. *Photonic Netw. Commun.* **2017**, *33*, 159–165. [CrossRef]
25. Parandin, F. Ultra-Compact and Low Delay Time All Optical Half Adder Based on Photonic Crystals. *Opt. Quantum Electron.* **2021**, *60*, 2275–2280.
26. Alanazi, A.K.; Alizadeh, S.M.; Nurgalieva, K.S.; Nesic, S.; Grimaldo Guerrero, J.W.; Abo-Dief, H.M.; Eftekhari-Zadeh, E.; Nazemi, E.; Narozhnyy, I.M. Application of neural network and time-domain feature extraction techniques for determining volumetric percentages and the type of two phase flow regimes independent of scale layer thickness. *Appl. Sci.* **2022**, *12*, 1336. [CrossRef]
27. Nazemi, E.; Roshani, G.; Feghhi, S.; Setayeshi, S.; Zadeh, E.E.; Fatehi, A. Optimization of a method for identifying the flow regime and measuring void fraction in a broad beam gamma-ray attenuation technique. *Int. J. Hydrog. Energy* **2016**, *41*, 7438–7444. [CrossRef]
28. Roshani, G.; Nazemi, E.; Roshani, M. Intelligent recognition of gas-oil-water three-phase flow regime and determination of volume fraction using radial basis function. *Flow Meas. Instrum.* **2017**, *54*, 39–45. [CrossRef]
29. Hosseini, S.; Taylan, O.; Abusurrah, M.; Akilan, T.; Nazemi, E.; Eftekhari-Zadeh, E.; Bano, F.; Roshani, G.H. Application of Wavelet Feature Extraction and Artificial Neural Networks for Improving the Performance of Gas–Liquid Two-Phase Flow Meters Used in Oil and Petrochemical Industries. *Polymers* **2021**, *13*, 3647. [CrossRef]
30. Nazemi, E.; Feghhi, S.; Roshani, G.; Peyvandi, R.G.; Setayeshi, S. Precise void fraction measurement in two-phase flows independent of the flow regime using gamma-ray attenuation. *Nucl. Eng. Technol.* **2016**, *48*, 64–71. [CrossRef]
31. Roshani, G.H.; Roshani, S.; Nazemi, E.; Roshani, S. Online measuring density of oil products in annular regime of gas-liquid two phase flows. *Measurement* **2018**, *129*, 296–301. [CrossRef]
32. Roshani, G.; Hanus, R.; Khazaei, A.; Zych, M.; Nazemi, E.; Mosorov, V. Density and velocity determination for single-phase flow based on radiotracer technique and neural networks. *Flow Meas. Instrum.* **2018**, *61*, 9–14. [CrossRef]
33. Roshani, S.; Azizian, J.; Roshani, S.; Jamshidi, M.B.; Parandin, F. Design of a miniaturized branch line microstrip coupler with a simple structure using artificial neural network. *Frequenz* **2022**, *76*, 255–263. [CrossRef]
34. Liu, A.; Leng, M.; Pan, G.; Yu, M. Automatic Coupler Design Based on Artificial Neural Network with Self-Adaptive Local Surrogates. *IEEE Trans. Microw. Theory Tech.* **2022**, *70*, 4711–4725. [CrossRef]
35. Parandin, F.; Reza Malmir, M. Reconfigurable all optical half adder and optical XOR and AND logic gates based on 2D photonic crystals. *Opt. Quantum Electron.* **2020**, *52*, 56. [CrossRef]
36. Jamshidi, M.B.; Lalbakhsh, A.; Mohamadzade, B.; Siahkamari, H.; Mousavi, S.M.H. A novel neural-based approach for design of microstrip filters. *AEU Int. J. Electron. Commun.* **2019**, *110*, 152847. [CrossRef]
37. Jamshidi, M.; Lalbakhsh, A.; Lotfi, S.; Siahkamari, H.; Mohamadzade, B.; Jalilian, J. A neuro-based approach to designing a Wilkinson power divider. *Int. J. RF Microw. Comput. Aided Eng.* **2020**, *30*, e22091. [CrossRef]
38. Yahya, S.I.; Alameri, B.M.; Jamshidi, M.B.; Roshani, S.; Chaudhary, M.A.; Ijemaru, G.K.; Mezaal, Y.S.; Roshani, S. A New Design Method for Class-E Power Amplifiers Using Artificial Intelligence Modeling for Wireless Power Transfer Applications. *Electronics* **2022**, *11*, 3608. [CrossRef]
39. Jamshidi, M.B.; Roshani, S.; Talla, J.; Roshani, S.; Peroutka, Z. Size reduction and performance improvement of a microstrip Wilkinson power divider using a hybrid design technique. *Sci. Rep.* **2021**, *11*, 7773. [CrossRef]
40. Du, R.-N.; Weng, Z.-B.; Zhang, C. A miniaturized filtering 3-dB branch-line hybrid coupler with wide suppression band. *Prog. Electromagn. Res. Lett.* **2018**, *73*, 83–89. [CrossRef]
41. Fardin, E.; Holland, A.; Ghorbani, K. Electronically tunable lumped element 90$^{circ} $ hybrid coupler. *Electron. Lett.* **2006**, *42*, 353–355. [CrossRef]
42. Beigizadeh, M.; Dehghani, R.; Nabavi, A. Analysis and design of a lumped-element hybrid coupler using limited quality factor of components. *AEU Int. J. Electron. Commun.* **2017**, *82*, 312–320. [CrossRef]
43. Abd El-Hameed, A.S.; Barakat, A.; Abdel-Rahman, A.B.; Allam, A. Design of low-loss coplanar transmission lines using distributed loading for millimeter-wave power divider/combiner applications in 0.18-μ m CMOS technology. *IEEE Trans. Microw. Theory Tech.* **2018**, *66*, 5221–5229. [CrossRef]
44. Pozar, D.M. *Microwave Engineering*; John Wiley & Sons: Hoboken, NJ, USA, 2011.
45. Zhang, F. Miniaturized and harmonics-rejected slow-wave branch-line coupler based on microstrip electromagnetic bandgap element. *Microw. Opt. Technol. Lett.* **2009**, *51*, 1080–1084. [CrossRef]
46. Wang, J.; Wang, B.-Z.; Guo, Y.-X.; Ong, L.; Xiao, S. A compact slow-wave microstrip branch-line coupler with high performance. *IEEE Microw. Wirel. Compon. Lett.* **2007**, *17*, 501–503. [CrossRef]
47. Lu, K.; Wang, G.-M.; Zhang, C.-X.; Wang, Y.-W. Design of miniaturized branch-line coupler based on novel spiral-based resonators. *J. Electromagn. Waves Appl.* **2011**, *25*, 2244–2253. [CrossRef]
48. Tsai, K.-Y.; Yang, H.-S.; Chen, J.-H.; Chen, Y.-J.E. A miniaturized 3 dB branch-line hybrid coupler with harmonics suppression. *IEEE Microw. Wirel. Compon. Lett.* **2011**, *21*, 537–539. [CrossRef]

49. Roshani, S.; Roshani, S. A compact coupler design using meandered line compact microstrip resonant cell (MLCMRC) and bended lines. *Wirel. Netw.* **2021**, *27*, 677–684. [CrossRef]
50. He, J.; Wang, B.-Z.; Shao, W.; Xiao, S.-Q. A Compact Microstrip Branch-Line Coupler with Capacitor Loading. In Proceedings of the 2008 IEEE MTT-S International Microwave Workshop Series on Art of Miniaturizing RF and Microwave Passive Components, Chengdu, China, 14–15 December 2008; pp. 139–141.
51. Roshani, S.; Yahya, S.I.; Roshani, S.; Rostami, M. Design and fabrication of a compact branch-line coupler using resonators with wide harmonics suppression band. *Electronics* **2022**, *11*, 793. [CrossRef]
52. Honari, M.M.; Mirzavand, R.; Mousavi, P.; Abdipour, A. Class of miniaturised/arbitrary power division ratio couplers with improved design flexibility. *IET Microw. Antennas Propag.* **2015**, *9*, 1066–1073. [CrossRef]
53. Kim, J.-S.; Kong, K.-B. Compact branch-line coupler for harmonic suppression. *Prog. Electromagn. Res. C* **2010**, *16*, 233–239. [CrossRef]
54. Gu, J.; Sun, X. Miniaturization and harmonic suppression rat-race coupler using C-SCMRC resonators with distributive equivalent circuit. *IEEE Microw. Wirel. Compon. Lett.* **2005**, *15*, 880–882.